An adaptive migration image-based CNN-based full waveform inversion (AIC-FWI)

Yulang Wu[1]*, *Hongyu Sun*[2], *Yapeng Tian*[3], *George A. McMechan*[3], *and Jing Zhou*[4]
[1] *Seattle Children's Hospital,* [2] *The University of Texas at El Paso,* [3] *The University of Texas at Dallas,* [4] *Amazon*

SUMMARY

We propose adaptive migration image-based CNN-FWI (AIC-FWI), an updated version of adaptive-feedback CNN-based reflection-waveform inversion (CNN-RWI), which trains a convolutional neural network (CNN) using the original velocity model and RTM image to predict the true velocity model. Unlike CNN-RWI, which requires high-resolution prior models, AIC-FWI captures features from migration images, making it suitable for inversion with a 1D velocity model. AIC-FWI offers several advantages: 1) no data fitting required, with higher-frequency data preferred; 2) self-supervised learning using pseudo-labels from the latest predicted models; 3) computational efficiency with fast convergence and scalability on GPUs/TPUs/CPU clusters. Synthetic tests on the Marmousi2 model show AIC-FWI can accurately predict velocity models from 1D initial models.

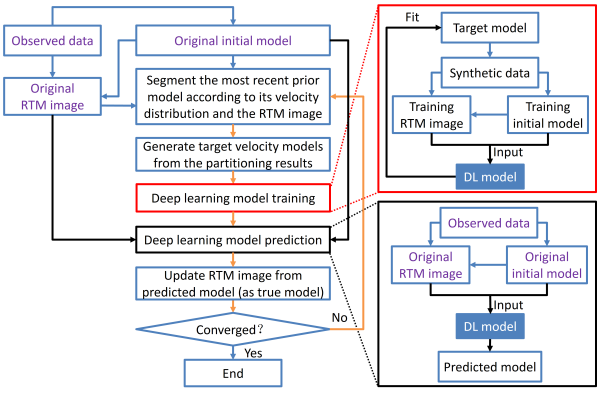

Figure 1: Flowchart of AIC-FWI.

INTRODUCTION

Full waveform-inversion (FWI) (Lailly, 1983; Tarantola, 1984; Gauthier et al., 1986; Mora et al., 1987; Crase et al., 1990; Pratt et al., 1998) is a non-linear optimization method to invert for a true velocity model by fitting synthetic data to observed data. In FWI, the velocity model is iteratively updated by the local gradient with background velocity information dominantly from refracted and turning waves and with interface information dominantly from reflected waves. Although the local gradient may contain the background velocity information from the reflected waves, it is relatively weaker than the interface location information, so the reflection-based background velocity information cannot be effectively applied to update the velocity model. Therefore, the background velocity in FWI is mainly updated by fitting refracted and turning waves, which, however, have limited penetration depth (Yao et al., 2020). Thus, conventional FWI mainly updates the shallow part of the velocity model by fitting refracted and turning waves. RWI has previously been used to recover the background velocity model using reflection data from the reflection-based gradient by separating tomography and migration information. Refer to Yao et al. (2020) for an overview of the separation of tomography and migration in reflection full waveform inversion.

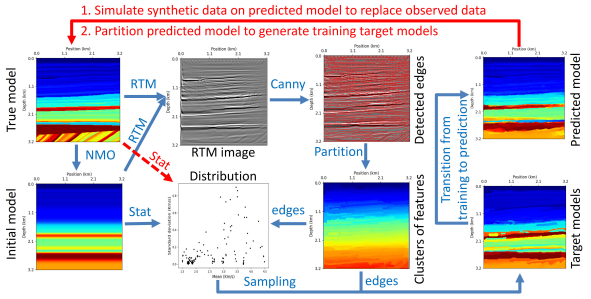

Figure 2: Workflow for adaptively generating training target velocity models (pseudo-labels). Blue arrows indicate the process of deriving pseudo-labels from the original initial velocity model and migration image. The solid red arrow represents the step where, after training the DL model to fit the target velocity models (only one example is shown), the predicted model replaces the unknown true velocity model as the 'synthetic true' model. This predicted model is then used to simulate synthetic data and obtain an updated migration image. After the first iteration, the predicted velocity model, rather than the original initial model, is partitioned to generate new training target models. It is important to note that this pipeline is solely for creating pseudo-labels and should not be confused with the original initial model and migration image, which are consistently used as inputs to the DL model for predicting the unknown true velocity model at each iteration.

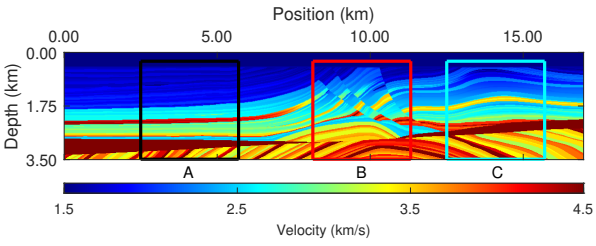

Figure 3: Three patches cropped from the Marmousi2 model: Model A, Model B, and Model C.

In recent years, convolutional neural networks (CNNs) have been extensively used in velocity inversion. Lewis and Vigh (2017) applied a CNN to extract features from seismic images of salt bodies, generating a prior model and a probability map for FWI. Several studies, including Araya-Polo et al. (2018),

10.1190/image2025-4316803.1

Wu and Lin (2019), Yang and Ma (2019), and Wang and Ma (2020), have leveraged CNNs to directly invert velocity models from raw seismic data, while Zhang and Gao (2021) used a CNN to infer velocity from migration images. Although these CNN-based approaches achieve end-to-end velocity estimation, they rely on the assumption that test models resemble the training dataset, ensuring an unbiased training process. However, in real-world applications, simplistic training and test models fail to capture the complexity of Earth's subsurface structures, leading to biased training data and severe overfitting.

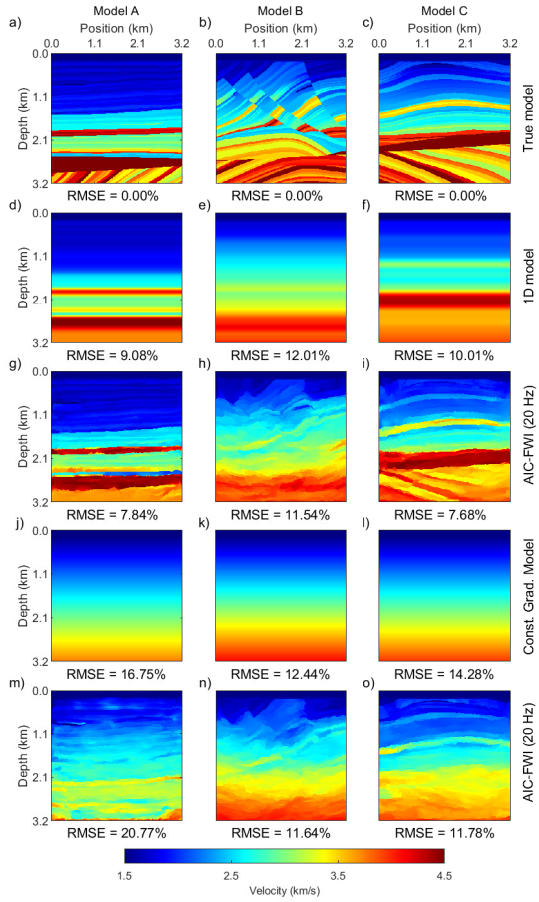

Figure 4: Comparison of velocity models. (a-c) are the true velocity models A, B, and C. (d-f) represent the corresponding 1D initial velocity models, derived by first computing the mean velocity at each depth and then applying a Gaussian filter for smoothing. (g-i) are the corresponding AIC-FWI-predicted velocity models, based on 1D initial velocity models in (d-f). (j-l) are the corresponding constant gradient initial velocity models. (m-o) are the AIC-FWI-predicted velocity models, based on constant gradient initial velocity models in (j-l).

To address this, deep learning has also been explored as a function approximator to re-parameterize a known smooth initial model and extract salient features that guide FWI. This approach helps regularize the inversion, focusing updates on the learned features (Wu and McMechan, 2018, 2019; Zhu et al., 2020; He and Wang, 2021). However, it still relies on data-fitting procedures, much like conventional FWI, and requires low-frequency data for stability.

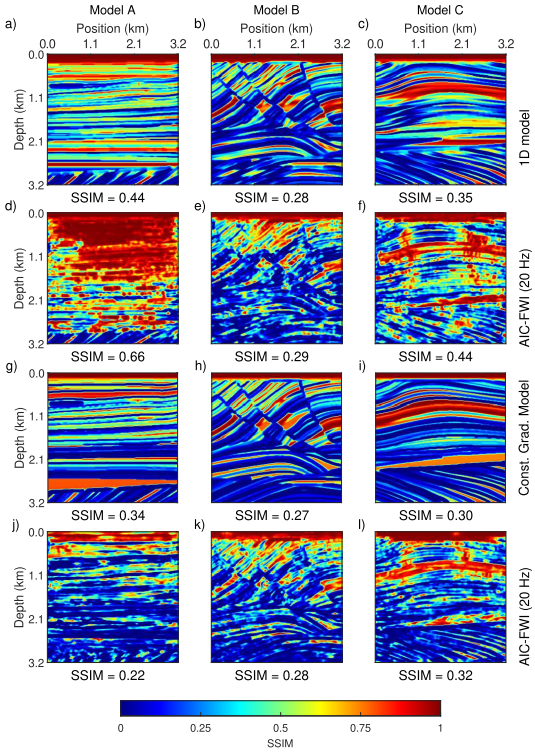

Figure 5: Structural Similarity Index Measure (SSIM) comparison for the velocity models in Figures 4d–4o, using true models A, B, and C in Figures 4a–4c as references.

An alternative physics-guided seismic inversion framework was introduced by Sun et al. (2020) and Wang et al. (2021), where forward modeling is reformulated within a recurrent neural network (RNN) framework. In this approach, inversion is treated as RNN training, leveraging automatic differentiation to accelerate optimization using deep learning platforms. Building on this, Sun et al. (2023) proposed Implicit Full Waveform Inversion (IFWI), incorporating deep neural representation (DNR) to replace conventional grid-based subsurface models with a continuous, coordinate-based representation. By avoiding grid discretization, IFWI overcomes the resolution limitations of traditional approaches. Notably, IFWI can converge from a random initial model toward the global minimum, recovering fine subsurface details that conventional FWI often fails to resolve due to local minima. However, representing high-frequency components remains challenging, and IFWI requires longer inversion times, particularly when initialized randomly.

Adaptive feedback convolutional neural network-based high-resolution reflection waveform inversion (CNN-RWI), proposed by Wu et al. (2022), predicts subsurface velocity models using an initial velocity model and its corresponding migration image. CNN-RWI is a self-supervised deep

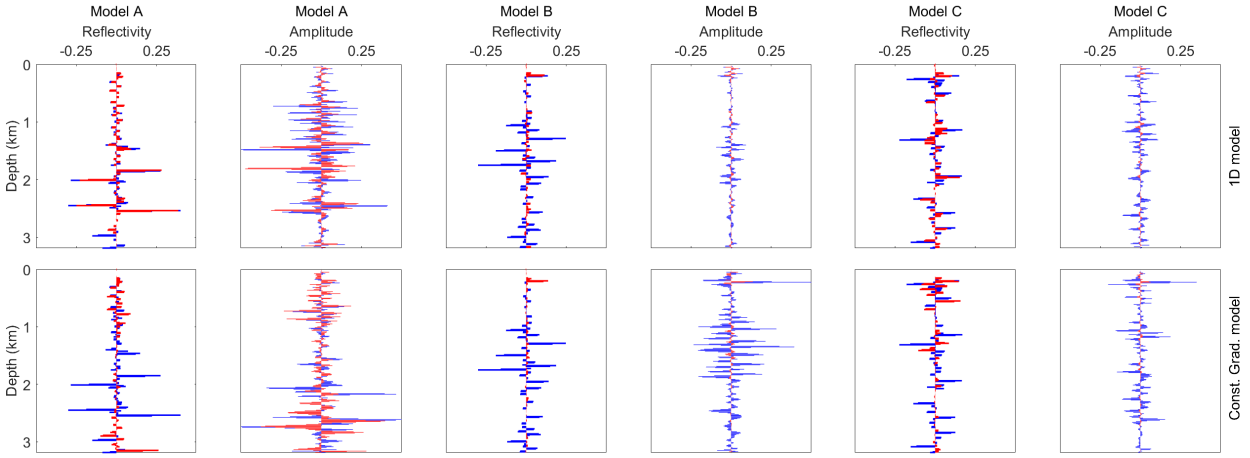

Figure 6: Comparison of velocity reflectivity profiles between true models (blue lines) and predicted models (red lines), as depicted in Figures 4 and 5, along with the corresponding migration traces at 1.6 km. Migration traces are extracted from migration images by using the true models (blue lines) or predicted models (red lines) as reference models for seismic data generation, while the respective (1D and constant gradient) initial models serve as migration models.

learning approach, as it iteratively generates a small set of pseudo-labels from the prior velocity model, eliminating the need for extensive, highly representative training datasets required by supervised deep learning and bypassing data fitting required in conventional FWI. During iterations, the pseudo-labels, derived by partitioning the most recent CNN-predicted velocity model, progressively improve in representation, enhancing the accuracy of CNN predictions and reducing overfitting. Unlike conventional FWI or physics-guided deep learning methods, CNN-RWI favors high-frequency seismic data, as it produces high-resolution migration images that enable the CNN to learn reflection interface locations and the velocities above and below them. However, CNN-RWI faces challenges, particularly its dependence on an accurate initial model to generate reliable pseudo-labels and the need for auto-tomography or migration velocity analysis (MVA) at each iteration for every training sample.

Building on the strengths and addressing the limitations of CNN-RWI, we introduce an adaptive migration image-based CNN-FWI (AIC-FWI), which enhances pseudo-label generation by partitioning initial models based on migration edges. This method incorporates the adaptive-feedback closed-loop mechanism from CNN-RWI to refine the inversion process further. Synthetic tests using various initial models—including 1D increasing velocity models and constant gradient velocity models on three windows of the Marmousi2 model demonstrate that AIC-FWI can efficiently and accurately predict velocity models, provided the initial velocity is not drastically different from the true velocity (e.g., constant gradient velocity models). Future work will focus on further testing and improving AIC-FWI to mitigate cycle-skipping issues and invert for complicated structures.

THEORY

Figure 1 illustrates the workflow of the proposed adaptive migration image-based CNN-FWI (AIC-FWI). The observed data is acquired from an unknown true velocity model. The initial model is generated through velocity analysis techniques such as NMO and the Dix formula, after which the original migration image is obtained via reverse-time migration (RTM) (Baysal et al., 1983; McMechan, 1983; Whitmore, 1983) using the initial model as the migration model. This initial velocity model and the RTM image are combined and fed into the deep learning model (DL model) to predict the unknown true velocity model (represented as the black box in Figure 1). A key challenge in AIC-FWI is training the DL model when representative velocity models similar to the unknown true velocity model are unavailable.

In adaptive-feedback CNN-RWI (Wu et al., 2022), the initial model (at the first iteration) and subsequent predicted models (CNN predictions at each iteration) are partitioned using the proposed spatially-constrained K-means clustering. This partitioning requires the initial model to have prominent features for clustering, which is a challenge in real-world applications. On the other hand, migration images derived from the initial models always contain substantial kinematic (spatial localization) and dynamic (amplitude and phase) information about reflectivity, which can be treated as key features in the image domain. Thus, AIC-FWI segments the initial or predicted models by applying the Canny edge detection algorithm (Canny, 1986) or template matching in Kilosort4 (Pachitariu, 2024) (a popular spike sorting toolbox in electrophysiological neuroscience) to identify edges and spikes in the migration images, respectively, which are then used to generate target velocity models as training pseudo-labels (Figure 2).

To prepare the input data in the training dataset (represented

as the red box in Figure 1), the synthetic seismic data is first obtained by forward modeling on the training target models, then the initial model and corresponding migration images are obtained using the same procedure as for the original initial model and migration image. This consistency in generating the training input data (initial models and migration images) is crucial in AIC-FWI. Even though the pseudo-labels (i.e., training target models) used for training may have different velocity distributions and structures compared to the unknown true velocity model, the mapping (i.e., the seismic processing) from the target data (training target models) to the input data (training initial model and migration image) remains consistent.

At the first iteration, the training target models derived from the partitioned original initial velocity model are biased relative to the unknown true velocity model because they have a different distribution. As a result, the trained DL model will have an algorithmic bias, leading to inaccurate predictions of the true velocity model at the first iteration (severe overfitting). Nevertheless, the predicted model can be more accurate than the input initial velocity model (even though it is less accurate than the predictions in the training), since the DL model has at least learned the consistent mapping in the biased distribution of the training target models. Therefore, as the predictions become more accurate, the DL model provides a more accurate predicted model, which, in turn, adaptively provides a less biased training dataset for the DL model training at the next iteration. In other words, the consistent mapping in both of the the training and prediction phases (represented as the red and black boxes respectively in Figure 1) enables the deep learning model to gradually align the distribution of training target models (pseudo-labels) with the unknown true velocity model, eliminating the need for a data-fitting optimization strategy as required in conventional FWI.

SYNTHETIC TEST

Three portions of the Marmousi2 P-wave velocity model (Martin et al., 2006) with a grid of 256×256 (Figure 3) are used to test the performance of AIC-FWI, with a 0.0125 km spatial sampling. To simulate observed data to calculate RTM images, 24 explosive Ricker-wavelet sources with a dominant frequency of 20 Hz are spaced every 0.288 km, and 256 receivers are spaced every 0.0125 km. All sources and receivers are at 0.0125km depth. The recording time is 4.0 s with a 1.0 ms sampling rate. We selected the Attention U-Net (Oktay et al., 2018) as the deep learning model. AIC-FWI generates 48 target models and obtains the corresponding RTM images in a parallel environment. The Attention U-Net is then trained to fit the training dataset over 1000 epochs (with 4 samples per minibatch) during each of the 20 iterations. Computational resources provided by ACCESS (TAMU ACES at Texas A&M University) are utilized for numerical simulations and deep learning (Boerner et al., 2023).

Figure 4 presents a comparison of velocity models inverted using AIC-FWI with two different initial velocity models: 1D initial velocity models (Figures 4d–4f) and constant gradient velocity models (Figures 4j–4l). Figure 5 shows the structural similarity index measure (SSIM) between the models in Figures 4d–4o and the true velocity models A, B, and C in Figures 4a–4c. Since the 1D initial velocity models (Figures 4d–4f) provide a more accurate mean velocity at each depth compared to the constant gradient initial models (Figures 4j–4l), the velocity models inverted by AIC-FWI from the 1D initial velocity models exhibit higher accuracy, as reflected in both RMSE and SSIM metrics.

Figures 4 and 5 also indicate that AIC-FWI struggles to recover Model B in both cases (1D and constant gradient initial models), likely due to the complexity and inaccuracy of the migration images, making it challenging for the deep learning model to learn the appropriate mapping. Figure 6 compares the velocity reflectivity profiles at 1.6 km for both true and predicted models from Figure 4, along with their corresponding migration traces. It is evident that the velocity reflectivity profiles and migration reflectivity interfaces in the predicted velocity models obtained from 1D initial models align more accurately in depth with those from true velocity models than those obtained using constant gradient initial models. This improved alignment in the velocity models corresponds to the dark red regions in the SSIM map shown in Figure 5. Figure 6 also demonstrates that, in comparison to the better alignment of reflectivities and migration amplitudes between true and predicted models A and C, both the velocity reflectivities and migration amplitudes of the predicted model B are significantly smaller than those of the true model B. Addressing the poorer performance with the constant gradient velocity model and handling complex velocity structures (e.g., model B) will be explored in future research.

CONCLUSIONS

The proposed AIC-FWI can efficiently and accurately predict a true velocity model based on a high-resolution RTM image and an inaccurate velocity model. The AIC-FWI inverts for the velocity model by iteratively shifting the distribution of the training velocity model set and the CNN-predicted velocity model towards the distribution of the true velocity model, without the need to minimize the data residuals or calculate the FWI model gradient.

ACKNOWLEDGMENTS

We appreciate Dr. Fuchun Gao for his valuable suggestions and feedback on this project. The research leading to this paper was supported by the Sponsors of The University of Texas at Dallas Geophysical Consortium. Hongyu Sun acknowledges UT System of STARs funds and UTEP University Research Institute Grant for funding. This work used TAMU ACES at Texas A&M University through allocation EES250028: Self-supervised Image-based Multi-parameter Inversion from the Advanced Cyberinfrastructure Coordination Ecosystem: Services & Support (ACCESS) program, which is supported by U.S. National Science Foundation grants #2138259, #2138286, #2138307, #2137603, and #2138296.

REFERENCES

Araya-Polo, M., J. Jennings, A. Adler, and T. Dahlke, 2018, Deep-learning tomography: The Leading Edge, **37**, no. 1, 58–66, doi: https://doi.org/10.1190/tle37010058.1.

Baysal, E., D. D. Kosloff, and J. W. Sherwood, 1983, Reverse time migration: Geophysics, **48**, no. 11, 1514–1524, doi: https://doi.org/10.1190/1.1441434.

Boerner, Timothy J., S. Deems, T. R. Furlani, S. L. Knuth, and J. Towns, 2023, ACCESS: Advancing Innovation: NSF's Advanced Cyberinfrastructure Coordination Ecosystem: Services & Support: In Practice and Experience in Advanced Research Computing (PEARC '23), July 23–27, 2023, Portland, OR, USA. ACM, New York, NY, USA, **4**pp., doi: https://doi.org/10.1145/3569951.3597559.

Canny, J., 1986, A computational approach to edge detection: IEEE Transactions on Pattern Analysis and Machine Intelligence, **8**, no. 6, 679–698, doi: https://doi.org/10.1109/TPAMI.1986.4767851.

Crase, E., A. Pica, M. Noble, J. McDonald, and A. Tarantola, 1990, Robust elastic nonlinear waveform inversion: Application to real data, Geophysics, **55**, 527–538, doi: https://doi.org/10.1190/1.1442864.

Gauthier, O., J. Virieux, and A. Tarantola, 1986, Two-dimensional nonlinear inversion of seismic waveforms: Numerical results: Geophysics, **51**, 1387–1403, doi: https://doi.org/10.1190/1.1442188.

Hewett, R. J., L. Demanet, and The PySIT Team, 2020, PySIT: Seismic imaging toolbox for Python: Zenodo.

Lailly, P., 1983, The seismic inverse problem as a sequence of before stack migrations: Conference on Inverse Scattering, Theory and Application, Society of Industrial and Applied Mathematics, Expanded Abstracts, 206–220.

Lewis, W. and D. Vigh, 2017, Deep learning prior models from seismic images for full-waveform inversion: 87th Annual International Meeting, SEG, Expanded Abstracts, 1512–1517, doi: https://doi.org/10.1190/segam2017-17627643.1.

McMechan, G. A., 1983, Migration by extrapolation of time-dependent boundary values: Geophysical Prospecting, **31**, 413–420, doi: https://doi.org/10.1111/j.1365-2478.1983.tb01060.x.

Martin, G. S., R. Wiley, and K. J. Marfurt, 2006, Marmousi2: An elastic upgrade for Marmousi: The Leading Edge, **25**, no. 2, 156–166, doi: https://doi.org/10.1190/1.2172306.

Mora, P., 1987, Nonlinear two-dimensional elastic inversion of multioffset seismic data: Geophysics, **52**, 1211–1228, doi: https://doi.org/10.1190/1.1442384.

Oktay, O., J. Schlemper, L. L. Folgoc, M. Lee, M. Heinrich, K. Misawa, K. Mori, S. McDonagh, N. Y. Hammerla, B. Kainz, and B. Glocker, 2018, Attention U-Net: Learning where to look for the pancreas: arXiv preprint, arXiv:1804.03999.

Pachitariu, M., S. Sridhar, J. Pennington, and C. Stringer, 2024 Spike sorting with Kilosort4: Nature Methods, **21**, no. 5, 914–921, doi: https://doi.org/10.1038/s41592-024-02232-7.

Pratt, R. G., C. Shin, and G. J. Hick, 1998, Gauss-Newton and full Newton methods in frequency space seismic waveform inversion: Geophysical Journal International, **133**, 341–362, doi: https://doi.org/10.1046/j.1365-246X.1998.00498.x.

Sun, J., Z. Niu, K. A. Innanen, J. Li, and D. O. Trad, 2020, A theory-guided deep-learning formulation and optimization of seismic waveform inversion, Geophysics, **85**, no. 2, R87–R99, doi: https://doi.org/10.1190/geo2019-0138.1

Sun, J., K. Innanen, T. Zhang, and D. Trad, 2023, Implicit seismic full waveform inversion with deep neural representation: Journal of Geophysical Research: Solid Earth, **128**, no. 3, e2022JB025964, doi: https://doi.org/10.1029/2022JB025964.

Tarantola, A., 1984, Inversion of seismic reflection data in the acoustic approximation: Geophysics, **49**, 1259–1266, doi: https://doi.org/10.1190/1.1441754.

Wang, W. and J. Ma, 2020, Velocity model building in a crosswell acquisition geometry with image-trained artificial neural networks: Geophysics, **85**, no. 2, U31–U46, doi: https://doi.org/10.1190/geo2018-0591.1.

Wang, W., G. A. McMechan, and J. Ma, 2021, Elastic isotropic and anisotropic full-waveform inversions using automatic differentiation for gradient calculations in a framework of recurrent neural networks: Geophysics, **86**, no. 6, R795–R810, doi: https://doi.org/10.1190/geo2020-0542.1.

Whitmore, N. D., 1983, Iterative depth migration by backward time propagation: 53rd Annual International Meeting, SEG, Expanded Abstracts, 382–385, doi: https://doi.org/10.1190/1.1893867.

Wu, Y. and Y. Lin, 2018, InversionNet: A real-time and accurate full waveform inversion with CNNs and continuous CRFs: arXiv:1811.07875.

Wu, Y., and G. A. McMechan, 2019, Parametric convolutional neural network-domain full-waveform inversion: Geophysics, **84**, R881–R896, doi: https://doi.org/10.1190/geo2018-0224.1.

Wu, Y., G. A. McMechan, and Y. Wang, 2022, Adaptive feedback convolutional-neural-network-based high-resolution reflection-waveform inversion: Journal of Geophysical Research: Solid Earth, **127**, e2022JB024138, doi: https://doi.org/10.1029/2022JB024138.

Yang, F., and J. Ma, 2019, Deep-learning inversion: A next-generation seismic velocity model building method: Geophysics, **84**, no. 4, R583–R599, doi: https://doi.org/10.1190/geo2018-0249.1.

Yao, G., D. Wu, and S. X. Wang, 2020, A review on reflection-waveform inversion: Petroleum Science, **17**, no. 2, 334–351, doi: https://doi.org/10.1007/s12182-020-00431-3.